MTOpen

Overexpressing Sonic Hedgehog Peptide Restores Periosteal Bone Formation in a Murine Bone Allograft Transplantation Model

Chunlan Huang[1], Minghui Tang[1], Eric Yehling[1] and Xinping Zhang[1]

[1]*Center for Musculoskeletal Research, University of Rochester, School of Medicine and Dentistry, Rochester, New York, USA*

Although activation of hedgehog (Hh) signaling has been shown to induce osteogenic differentiation *in vitro* and bone formation *in vivo*, the underlying mechanisms and the potential use of Hh-activated mesenchymal progenitors in bone defect repair remain elusive. In this study, we demonstrated that implantation of periosteal-derived mesenchymal progenitor cells (PDMPCs) that overexpressed an N-terminal sonic hedgehog peptide (ShhN) via an adenoviral vector (Ad-ShhN) restored periosteal bone collar formation in a 4-mm segmental bone allograft model in immunodeficient mice. Ad-ShhN enhanced donor cell survival and microvessel formation in collagen scaffold at 2 weeks after surgery and induced donor cell–dependent bone formation at 6 weeks after surgery. Fluorescence-activated cell sorting analysis further showed that Ad-ShhN-PDMPC–seeded scaffold contained a twofold more $CD45^{-}Sca\text{-}1^{+}CD34^{+}VEGFR2^{+}$ endothelial progenitors than Ad-LacZ-PDMPC–seeded scaffold at day 7 after surgery. Ad-ShhN–transduced PDMPCs induced a 1.8-fold more $CD31^{+}$ microvessel formation than Ad-LacZ–transduced PDMPCs in a coculture of endothelial progenitors and PDMPCs. Taken together, our data show that overexpression of ShhN in mesenchymal progenitors improves bone defect reconstruction by enhancing donor progenitor cell survival, differentiation, and scaffold revascularization at the site of compromised periosteum. Hh agonist–based therapy, therefore, merits further investigation in tissue engineering–based applications aimed at enhancing bone defect repair and reconstruction.

Received 24 May 2013; accepted 20 September 2013; advance online publication 24 December 2013. doi:10.1038/mt.2013.222

INTRODUCTION

Repair and reconstruction of large bone defects remain a challenging clinical problem. Current management of bone defect repair often involves the use of bone graft materials. Each year more than 500,000 bone graft procedures are performed in the United States, and more than 2.2 million are performed annually worldwide.[1] Although an autograft is considered as the "gold standard," the use of an autograft is limited due to its associated donor site morbidity and the restricted availability for large bone defect repair. Compared with autografts, allografts are often available in desired size, shape, and quantity. Cortical bone allografts further provide immediate support for structural bone defect reconstruction. However, due to the absence of osteogenic cells, bone allografts are inferior in new bone induction and revascularization. A 10-year failure rate of cortical allograft transplantations is reported at 60% due to nonunions, infection, and propagation of microdamages in devitalized bone.[2,3] A novel approach to revitalize structural bone allografts has been proposed.[4] The approach centers on engraftment of bone-forming cells around bone allografts, mimicking periosteal response in autograft repair.[5–9] The key to the success of this approach is to create a tissue-engineered periosteum replacement carrying osteogenic and angiogenic signals capable of recapitulating the effective repair elicited by periosteum.

To the end of identifying critical osteogenic and angiogenic signals underlying periosteum-initiated repair and reconstruction, we recently isolated a population of mesenchymal progenitor cells from the healing autograft periosteum (PDMPCs). These cells express typical MPC markers such as Sca-1, SSEA4, CD105, and CD140b. They can further give rise to multiple cell types, such as osteoblasts, chondrocytes, and adipocytes *in vitro*. Examination of the osteogenic differentiation of these cells shows that activation of Hh pathway leads to marked induction of osteoblasts *in vitro* and copious bone formation *in vivo*. Using a loss-of-function approach to delete the receptor of all Hh ligands, smoothened-1, we further show that Hh activation is required for effective periosteum-dependent bone graft repair and reconstruction.[10]

As a family of key morphogens in embryonic development, hedgehogs, such as Indian hedgehog (Ihh) and Sonic hedgehog (Shh), are known to play key roles in skeletal formation and osteoblast development.[11] Both Ihh and Shh have been shown to induce osteogenic differentiation of MPC lines through induction of RUNX2, an essential transcriptional factor for osteoblast differentiation and bone formation.[12] In addition to bone formation, the hedgehog pathway has also been intimately linked to vascular formation and angiogenesis.[13] Ihh is implicated in blood island formation and early yolk sac angiogenesis,[14] whereas Shh is critical for the assembly of angioblasts (endothelial precursors) into blood vessel network, a process known as vasculogenesis during

The first two authors contributed equally to this work.

Correspondence: *Xinping Zhang, Center for Musculoskeletal Research, University of Rochester Medical Center, 601 Elmwood Avenue, Rochester, New York 14642, USA. E-mail: xinping_zhang@urmc.rochester.edu*

embryonic development.[15,16] Hedgehog signaling is active in adult coronary vasculature, and disruption of Hh signaling led to loss of coronary blood vessels and subsequent cardiomyocyte cell death in mice.[17] The hedgehog signaling is induced during injury and in ischemic tissues. Delivery of Shh improves the repair of ischemic myocardium by promoting angiogenesis and microvascular remodeling.[18–20]

The combined effects of hedgehog on osteogenesis and angiogenesis warrant further investigation for the use of Hh agonists in bone defect repair and reconstruction. To this end, we used an *ex vivo* hedgehog gene therapy approach and implanted PDMPCs that overexpressed an N-terminal peptide of human sonic hedgehog (ShhN) around a devitalized bone allograft via a collagen scaffold. The treated allograft was used to repair a 4-mm segmental defect created in the immunodeficient mouse femurs. Our results demonstrated that overexpression of ShhN in periosteal cells markedly enhanced donor cell survival and revascularization of the scaffold at the site of repair, leading to a complete restoration of periosteal bone formation around bone allografts.

RESULTS

Implantation of ShhN-overexpressing PDMPCs restores periosteal bone collar formation around devitalized bone allografts

The effects of ShhN on osteogenic differentiation of PDMPCs were examined. Adenovirus-mediated gene transduction led to ~45,000-fold induction of human *ShhN* gene expression in PDMPCs (**Figure 1a**). Overexpression of *ShhN* markedly enhanced osteogenic differentiation of PDMPCs as evidenced by enhanced alkaline phosphatase staining (**Figure 1b**) and increased expression of osteogenic genes such as *RUNX2* and *osteocalcin* (**Figure 1c**,**d**). Overexpression of *ShhN* further enhanced the level of RUNX2 protein in the western blot analyses (**Supplementary Figure S1**). In addition to the enhanced expression of osteogenic genes, a strong induction of angiogenic genes such as *ANG1*, *ANG2*, *ANG4,* and *VEGF* was also observed in cells transduced with Ad-ShhN (**Figure 1e**–**h**).

To enable tracking of the donor cells, PDMPCs were isolated from green fluorescence protein (GFP)–transgenic mice. Adenoviral transduced PDMPCs were loaded onto collagen scaffolds and wrapped around devitalized bone allografts in immunodeficient mice. Healing of the allografts treated with Ad-ShhN-PDMPCs or Ad-GFP-PDMPCs was examined. X-ray analyses showed limited bone callus formation at the host side of cortical bone junction in allografts treated with Ad-GFP-PDMPCs 6 weeks following implantation. By contrast, in allografts treated with Ad-ShhN-PDMPCs, a complete bridging callus was observed around the bone allograft (**Figure 2a**). MicroCT 3D reconstruction of the allograft at 6 weeks showed that the allograft engrafted with Shh-overexpressing PDMPCs formed a contiguous periosteal collar bone callus around allograft (**Figure 2b**, top panel). Quantitative volumetric analyses showed a 4.6-, 2.5, and 3.5-fold increase of new bone formation at the donor site, the host site, and the total callus, respectively, in Ad-ShhN-PDMPC–treated allografts as compared with the control Ad-GFP-PDMPC–treated allografts (**Figure 2c**; $P < 0.05$; $n = 6$).

Histologic analyses showed that Ad-GFP-PDMPC–treated allograft had minimal periosteal bone formation at the donor site, with persistent collagen scaffold around allograft (**Figure 2d**, *indicates scaffold). By contrast, Ad-ShhN-PDMPC–treated allograft formed a contiguous bone callus across the entire length of the donor bone (**Figure 2e**, indicated by arrows). The scaffold was largely absorbed and the callus was reconstituted with bone marrow. Histomorphometric analyses at 6 weeks showed a 4.6-fold increase in bone formation and a 3.5-fold decrease in fibrotic tissue at the donor site (**Figure 2f**; $P < 0.05$; $n = 6$). In the host side callus, bone formation was increased by 35% and fibrotic issue was reduced by 63% in Ad-ShhN-PDMPC–treated allografts (**Figure 2g**; $P < 0.05$; $n = 6$). Persistent cartilage observed at the cortical bone junction in the control allografts was completely eliminated in Ad-ShhN-PDMPC–treated allografts (**Figures 2f**,**g**; $P < 0.05$; $n = 6$).

ShhN overexpression promotes neovascularization, enhanced donor cell survival, and donor cell–dependent bone formation

GFP^+ donor cells were tracked at the repair sites for a period of 6 weeks using immunohistochemistry. In Ad-GFP-PDMPC–treated allografts, only a small number of donor progenitor cells were detected in collagen scaffold at 2 weeks (**Figure 3a**,**e**,**i**,**m**). Most of the cells were found at the cortical bone junction or close to the surface of the scaffold (**Figure 3a**,**i**). A few of the donor cells were incorporated into bone and cartilage tissues at the cortical bone junction (**Figure 3e**,**i**, arrow in i). Sparsely distributed cells were found in the scaffold further away from the junction (**Figure 3m**). By contrast, in Ad-ShhN-PDMPC–treated allografts, abundant GFP^+ cells were found throughout the collagen scaffold at 2 weeks after surgery (**Figure 3b**,**f**,**j**,**n**). At a higher magnification, dense GFP^+ cellular layers were observed in the scaffold (**Figure 3j**). By 6 weeks, abundant GFP^+ cells were found to be incorporated into the new bone matrix at the donor site (**Figure 3h**,**l**). At a higher magnification, GFP^+ osteocytes and osteoblasts were readily identified along new bone surface and within bone matrix in the periosteal callus (**Figure 3p**, arrows). By contrast, in Ad-GFP-PDMPC–treated allografts (**Figure 3c**,**g**,**k**,**o**), GFP^+ cells were found scattered within the scaffold at the donor site (**Figure 3k**). A few of them were found embedded within poorly differentiated cartilage tissue (**Figure 3k**, arrow). At a higher magnification, the majority of GFP^+ cells in the collagen scaffold were seen as undifferentiated elongated fibroblastic cells (**Figure 3o**). No GFP^+ osteoblasts or osteocytes were identified in the densely packed scaffold.

Microvessel formation within the collagen scaffold was examined. Immunohistochemical staining of CD31 demonstrated a marked increase in $CD31^+$ microvessel formation in Ad-ShhN-PDMPC–seeded scaffold as compared with the control Ad-GFP-PDMPC–seeded scaffold at 2 weeks after implantation (**Figure 4a**,**c** vs. **4b**,**d**). Many of the vessels found in Ad-ShhN-PDMPC scaffold had larger, more mature lumens containing red blood cells (**Figure 4d**, arrows). Quantification of the numbers of microvessels within the scaffold showed a threefold increase in Ad-ShhN-PDMPC scaffold as compared with the control (**Figure 4g**; $P < 0.05$; $n = 4$). With enhanced vascularity, $TRAP^+$ cells were also found to be increased within collagen scaffold (**Figure 4e**,**f**). Quantification analyses showed a 10-fold increase in the number of $TRAP^+$ cells in Ad-ShhN-PDMPC scaffold as compared with the control (**Figure 4h**; $P < 0.05$; $n = 4$).

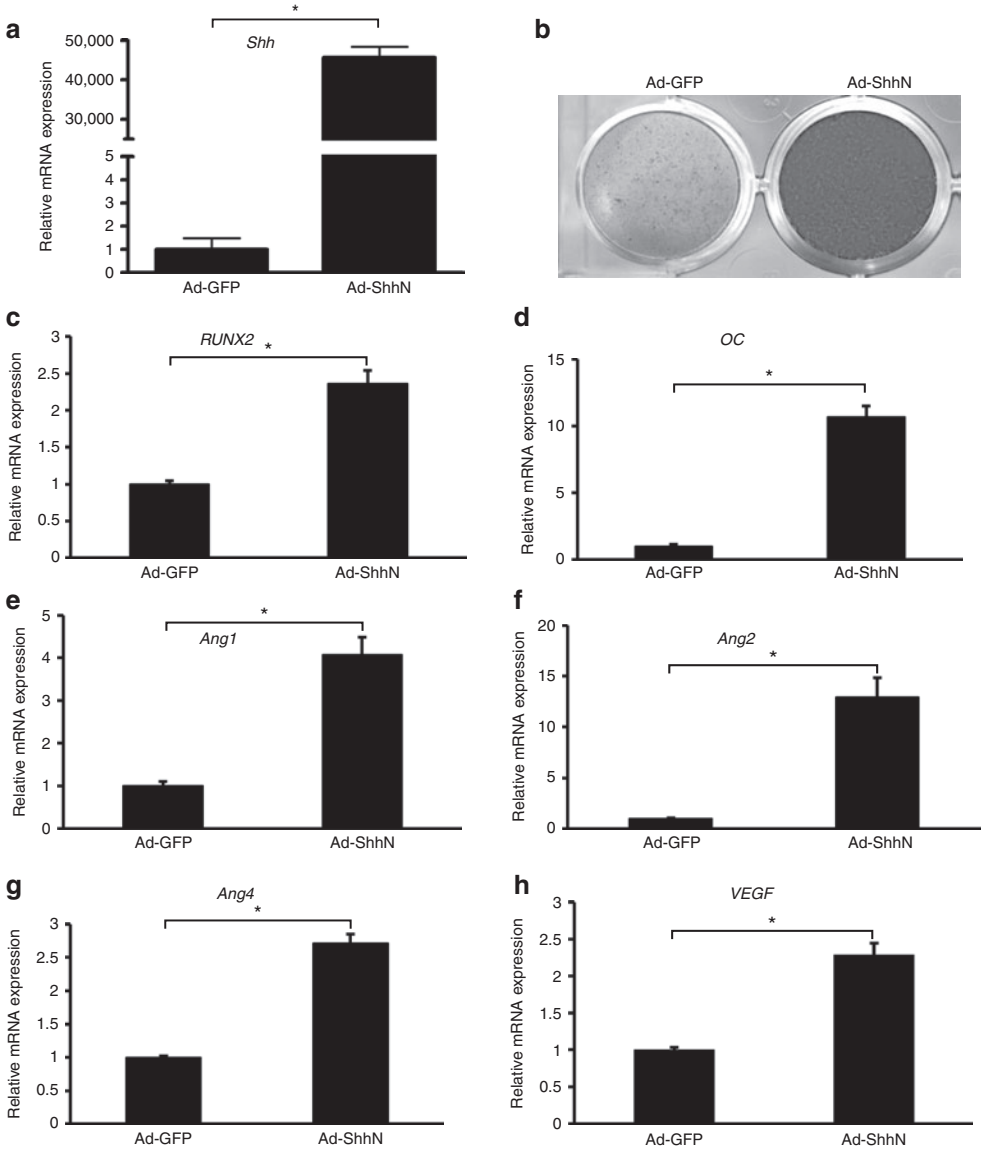

Figure 1 Induction of osteoblastic differentiation of periosteal-derived mesenchymal progenitor cells (PDMPCs) by N-terminal sonic hedgehog peptide (ShhN) via an adenoviral vector (Ad-ShhN). (**a**) Reverse transcriptase–polymerase chain reaction analyses demonstrate strong induction of the transgene *ShhN* in PDMPCs transduced with Ad-ShhN. (**b**) Marked induction of osteogenic differentiation of ShhN-overexpressing PDMPCs is shown by alkaline phosphatase staining, and (**c**) osteogenic and angiogenic gene expression at day 7 (C–H). All gene expressions were normalized to β-actin and presented as relative to that observed in cells transduced with adenovirus-containing green fluorescent protein (Ad-GFP) or Ad-ShhN.

ShhN overexpression enhances revascularization of collagen scaffold through promotion of the morphogenesis of endothelial progenitors from the peripheral tissues, such as skeletal muscles and fat

The rapid induction of microvessel formation in Ad-ShhN-PDMPC scaffold prompted us to investigate the potential effects of ShhN on recruitment and morphogenesis of endothelial progenitors from the surrounding tissues of periosteum, such as skeletal muscles or subcutaneous fat. It has been shown that both tissues contained abundant endothelial progenitors.[21,22] To determine whether ShhN could recruit more endothelial progenitors into the scaffold and further enhanced the assembly of microvessels, we first characterized different fractions of mononuclear cells isolated from muscle and fat using fluorescence-activated cell sorting (FACS). Culturing of different fractions of the mononuclear cells from muscle and fat in Matrigel showed that $CD45^{-}Sca\text{-}1^{+}CD34^{+}$ and $CD45^{-}Sca\text{-}1^{+}CD34^{+}VEGFR2^{+}$ cells were capable of forming abundant and robust $CD31^{+}$ microvessels *in vitro* (**Supplementary Figure S3** and **Figure 5a2, b2**). FACS analyses showed that muscle and fat contained an average of 7.7 and 5.8% $CD45^{-}Sca\text{-}1^{+}CD34^{+}VEGFR2^{+}$ endothelial progenitors, respectively, in the mononuclear cell preps (**Figure 5a1,b1**, arrows). In comparison, fewer $CD45^{-}Sca\text{-}1^{+}CD34^{+}VEGFR2^{+}$ cells were identified in bone marrow (**Supplementary Figure S2**).

Next we examined the frequency of $CD45^{-}Sca\text{-}1^{+}CD34^{+}VEGFR2^{+}$ endothelial progenitor cells in Ad-LacZ-PDMPC– or Ad-ShhN-PDMPC–seeded collagen scaffold at

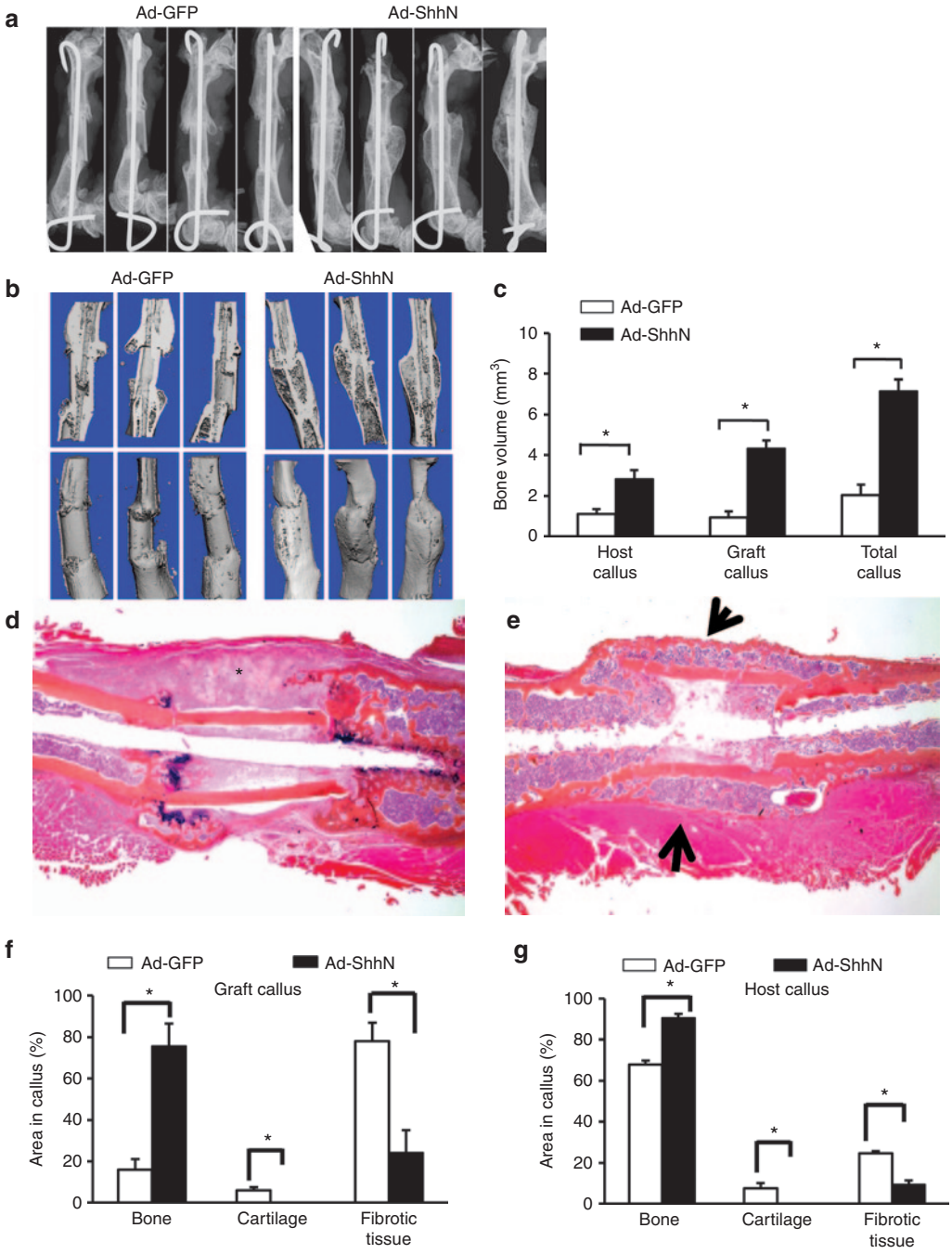

Figure 2 Overexpression of ShhN in periosteal-derived mesenchymal progenitor cells (PDMPCs) restores periosteal bone formation in segmental allograft transplantation model. (**a**) X-ray and (**b**) MicroCT imaging show marked induction of periosteal bone callus formation in Ad-ShhN-PDMPC–treated allografts at 6 weeks following implantation. (**c**) Quantitative analyses show enhanced bone volume at host side and graft side. $n = 6$; $^*P < 0.05$. (**d**) Histology shows poor osseointegration at the cortical bone junctions in allografts engrafted with Ad-GFP-PDMPCs. Collagen scaffold (indicated with *) persists at the site of implantation. By contrast, (**e**) in allografts treated with Ad-ShhN-PDMPCs, periosteal collar bone (arrows) was restored across the entire length of allograft with near complete reconstitution of bone marrow in the callus. Quantitative histomorphometric analyses further illustrate increased bone formation and decreased fibrotic tissue in allografts treated with Ad-ShhN-PDMPCs at (**f**) the donor side and (**g**) host site. $n = 6$; $^*P < 0.05$. Ad-GFP, adenovirus-containing green fluorescent protein; AD-ShhN, N-terminal sonic hedgehog peptide via an adenoviral vector.

day 7 following surgical implantation. FACS analyses show that Ad-ShhN-PDMPC scaffold contained a 2.4-, 1.8-, and 2.1-fold more $CD45^-CD34^+VEGFR2^+$, $CD45^-Sca\text{-}1^+VEGFR2^+$, or $CD45^-Sca\text{-}1^+CD34^+VEGFR2^+$ endothelial progenitors than Ad-LacZ-PDMPC scaffold (**Figure 6a**,**b**; $P < 0.05$; $n = 3$). To determine whether ShhN overexpression could affect the differentiation and morphogenesis of the endothelial progenitors from the peripheral tissues, we cocultured $CD45^-Sca\text{-}1^+CD34^+$ endothelial progenitor cells with Ad-ShhN-PDMPCs. Our data showed that Ad-ShhN–transduced PDMPCs significantly increased $CD31^+$ microvessel formation by 1.8-fold as compared with the control Ad-LacZ-PMDPCs (**Figure 6e**; $n = 4$; $P < 0.05$). Compared with

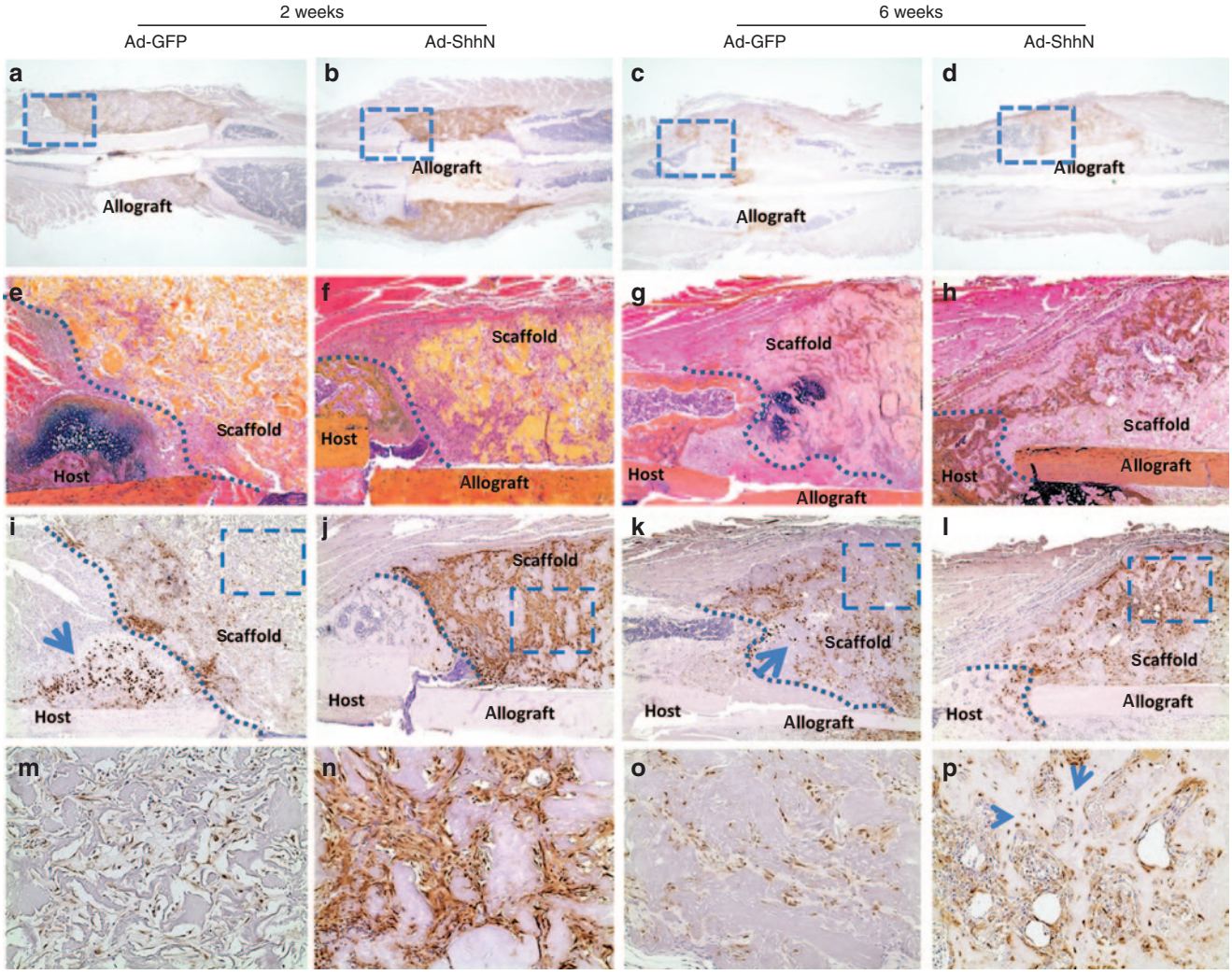

Figure 3 Overexpression of ShhN enhances survival and osteogenic differentiation of the donor periosteal-derived mesenchymal progenitor cells (PDMPCs). PDMPCs were isolated from green fluorescent protein (GFP) transgenic mice. Cells transduced with (**a**,**e**,**i**,**m**,**c**,**g**,**k**,**o**) Ad-GFP or (**b**,**f**,**j**,**n**,**d**,**h**,**l**,**p**) Ad-ShhN were implanted around bone allografts. GFP immunohistochemical staining was performed on samples harvested at (**a**,**b**,**e**,**f**,**i**,**j**,**m**,**n**) 2 weeks and (**c**,**d**,**g**,**h**,**k**,**l**,**o**,**p**) 6 weeks after implantation (original magnification × 1.25). Boxed regions in **a**–**d** are illustrated at a higher magnification (original magnification × 10) in **e**–**h**) for H&E/Alcian Blue staining and **i**–**l** for GFP immunohistochemistry. Host and donor sites are marked by dashed line in **e**–**h** and **i**–**l**. Of note are the formation of dense layers of GFP^+ cells at 2 weeks (F&J) and induction of bone formation at 6 weeks (H&L) in Ad-ShhN-PDMPC–treated allograft. In control PDMPC-treated allograft, GFP^+ cells are sparsely distributed at the cortical bone junctions or incorporated into host cartilaginous callus at 2 weeks (arrow in **i**) and 6 weeks (arrow in **k**). Boxed regions in **i**–**l** are further illustrated at original magnification × 40 in **m**–**p**, respectively. In (**n**) Ad-ShhN-PDMPC–seeded collagen scaffold, GFP^+ cells are densely repopulated as compared with (**m**) the Ad-GFP-PDMPC–seeded collagen scaffold at 2 weeks. By 6 weeks, abundant GFP^+ cells are shown embedded within bone matrix and along new bone surface (arrows in **p**) in Ad-ShhN-PDMPC–treated allograft. (**d**) In the control allografts, the majority of GFP^+ cells remain undifferentiated and are shown trapped in the scaffold. Ad-GFP, adenovirus-containing GFP; Ad-ShhN, N-terminal sonic hedgehog peptide via an adenoviral vector.

the controls, Ad-ShhN–transduced cells visibly induced the formation of more microvessel branches with more complex morphology and network *in vitro* (**Figure 6c,d**).

DISCUSSION

To exploit the use of hedgehog agonist as an osteogenic and angiogenic agent for bone defect repair and reconstruction, in this study, we used an *ex vivo* gene therapy approach overexpressing an N-terminal peptide of human Shh in PDMPCs. To determine the efficacy of progenitor cell-based gene therapy, an immune-deficient mouse model was used to test the effects of ShhN on donor and host cells. Ad-GFP-PDMPC–treated devitalized allografts showed absence of periosteal bone formation and poor osseointegration at the cortical bone junctions, similar to allograft transplantation in immunocompetent mice.[5,6,23] By contrast, Ad-ShhN-PDMPC–treated allografts completely restored periosteal collar bone formation and markedly improved osseointegration of the allografted bone. Further analyses showed that ShhN significantly enhanced donor cell survival and donor cell–dependent bone formation at the site of repair. ShhN additionally promoted the recruitment and morphogenesis of peripheral endothelial progenitors, leading to rapid revascularization of the cellular scaffold.

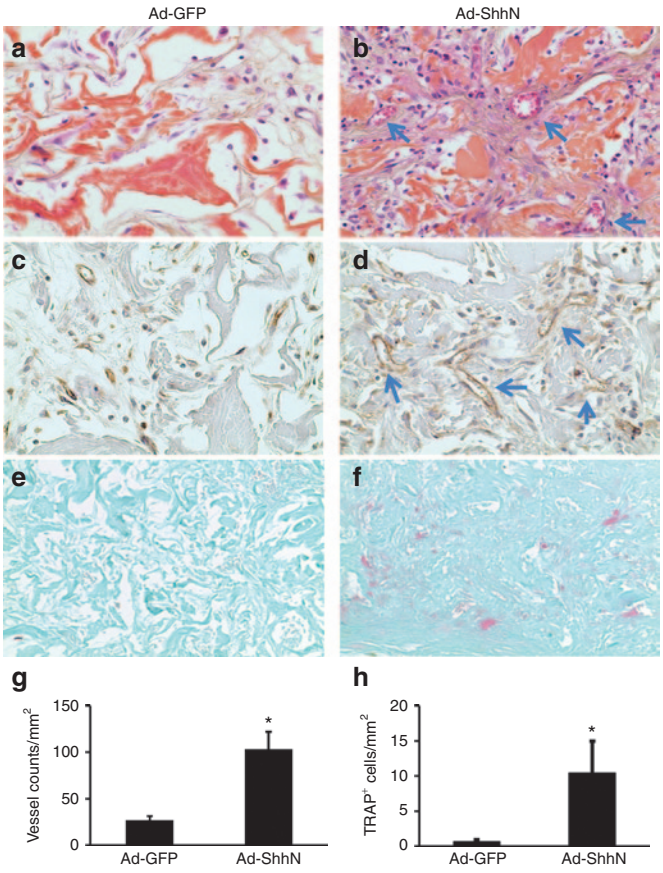

Figure 4 ShhN enhances rapid revascularization of periosteal-derived mesenchymal progenitor cell (PDMPC) collagen scaffold *in vivo*. (**a**,**b**) H&E and (**c**,**d**) immunohistochemical staining of $CD31^+$ vessels show enhanced microvessel formation in (**b**,**d**) Ad-ShhN-PDMPC–seeded collagen scaffolds as compared with (**a**,**c**) the controls at 2 weeks after surgery. TRAP staining shows more $TRAP^+$ cells in (**f**) Ad-ShhN-PDMPC–seeded scaffolds than (**e**) the controls. Quantitative analyses of (**g**) microvessels and (**h**) $TRAP^+$ cells in the scaffold are illustrated. $n = 4$; $^*P < 0.05$. Ad-GFP, adenovirus-containing GFP; Ad-ShhN, N-terminal sonic hedgehog peptide via an adenoviral vector.

Hedgehog pathway is essential for long bone development and perichondral collar bone formation.[24,25] Our previous study further shows that Hedgehog pathway is required for postnatal long bone defect healing that implicates periosteum.[10] By implantation of PDMPCs overexpressing ShhN in a bone allograft model, here we provide further evidence to show that activation of Hh pathway in MPCs effectively enhances long bone defect repair and reconstruction. By tracking the donor cell fate for a period of 6 weeks, we demonstrated that ShhN markedly enhanced donor cell survival, repopulation, and differentiation in the scaffold. Without ShhN stimulation, only a few PDMPCs survived in the scaffold, with a small proportion of the cells incorporated into cartilage or bone at the cortical bone junction. The majority of the donor PDMPCs remained as undifferentiated fibroblastic cells in the scaffold at 6 weeks after implantation. By contrast, ShhN-transduced PDMPCs exhibited better survival capability and quickly repopulated the scaffold, with a large number of cells differentiating into osteoblasts and participating in collar bone formation at the donor site (**Figure 3**). In addition to the direct effects on donor cells, our data also showed that Ad-ShhN-PDMPC treatment enhanced host bone callus formation, suggesting a paracrine effect of ShhN on host progenitor cells. In the allografts treated with control PDMPC, persistent cartilaginous tissue was observed at the cortical bone junction 6 weeks after surgery (**Figure 3g**). By contrast, the persistent cartilaginous tissue was eliminated from the host and donor callus in Ad-ShhN-PDMPC–treated allografts, indicating an improved endochondral bone formation at the cortical bone junction. As a result of the elimination of the residue cartilage, Ad-ShhN-PDMPC–treated allografts demonstrated better osseointegration at the cortical bone junction. Indeed, due to the lack of a cholesterol-binding site, ShhN peptide is shown to be able to diffuse to a greater distance than the native protein.[26] This unique property of ShhN favors postnatal repair, which is less dependent on a morphogen gradient. Similar to *ShhN*, a number of therapeutic genes, such as *BMPs* and *VEGF*, have been previously demonstrated to elicit both paracrine and autocrine effects on repair of large bone defect.[6,27,28]

Besides enhancing cellular survival and differentiation, our data further showed that Hh overexpression induced rapid revascularization of the scaffold at the site of repair. The enhanced neovascularization is associated with the induction of several key angiogenic gene expression, such as *VEGF*, *ANG1*, *ANG2*, and *ANG4* in PDMPCs (**Figure 1**). VEGF signaling is linked with Hh pathways in vascular patterning.[16,29] In addition to VEGF, Hh signaling is also known to regulate both *ANG1* and *ANG2*.[30,31] ANG1 promotes angiogenesis and arteriogenesis, whereas both ANG2 and ANG4 are classified as antagonists of ANG1-Tie2 signaling during development. However, despite an antagonizing role of ANG2 during development, recent data have shown that ANG2 is required for postnatal remodeling of the vessels.[32] ANG2 can further exert proangiogenic functions and enhance vessel sprouting in a Tie2-independent manner via activation of integrins/focal adhesion kinase signaling in endothelial tip cells.[33] The function of ANG4 is less well studied. Nevertheless, it is shown that ANG4 can induce angiogenesis *in vivo* in the mouse corneal micropocket assays.[34] Future experiments are needed to establish the role of angiopoietin genes in Hh-induced neovascularization.

In addition to the induction of angiogenic factors by ShhN, our current data further suggest a novel mechanism that involves the recruitment of endothelial progenitors from the peripheral tissues such as fat and muscles. It has been shown that exogenous administration of Shh accelerates the repair of ischemic myocardium by enhancing the recruitment of bone marrow–derived endothelial progenitor cells to the injury site.[35] A similar mechanism is further noted in diabetic skin wound closure treated with Shh protein.[36] By comparing the frequency of endothelial progenitors from bone marrow, muscle, and fat, we found that bone marrow contained fewer endothelial progenitors than muscles and subcutaneous fat[22] (**Supplementary Figure S2**). By contrast, $CD45^-CD34^+Sca\text{-}1^+VEGFR2^+$ cells constituted 5–10% of the isolated mononuclear cell populations in muscle and fat. The presence of abundant endothelial progenitors in surrounding soft tissues suggests the potential involvement of these cells in rapid vascularization of the scaffold. In support of this notion, we provided evidence to show that Ad-ShhN-PDMPC scaffold contained more $CD45^-CD34^+Sca\text{-}1^+VEGFR2^+$ endothelial progenitor cells than Ad-LacZ-PDMPC scaffold at day 7 after transplantation

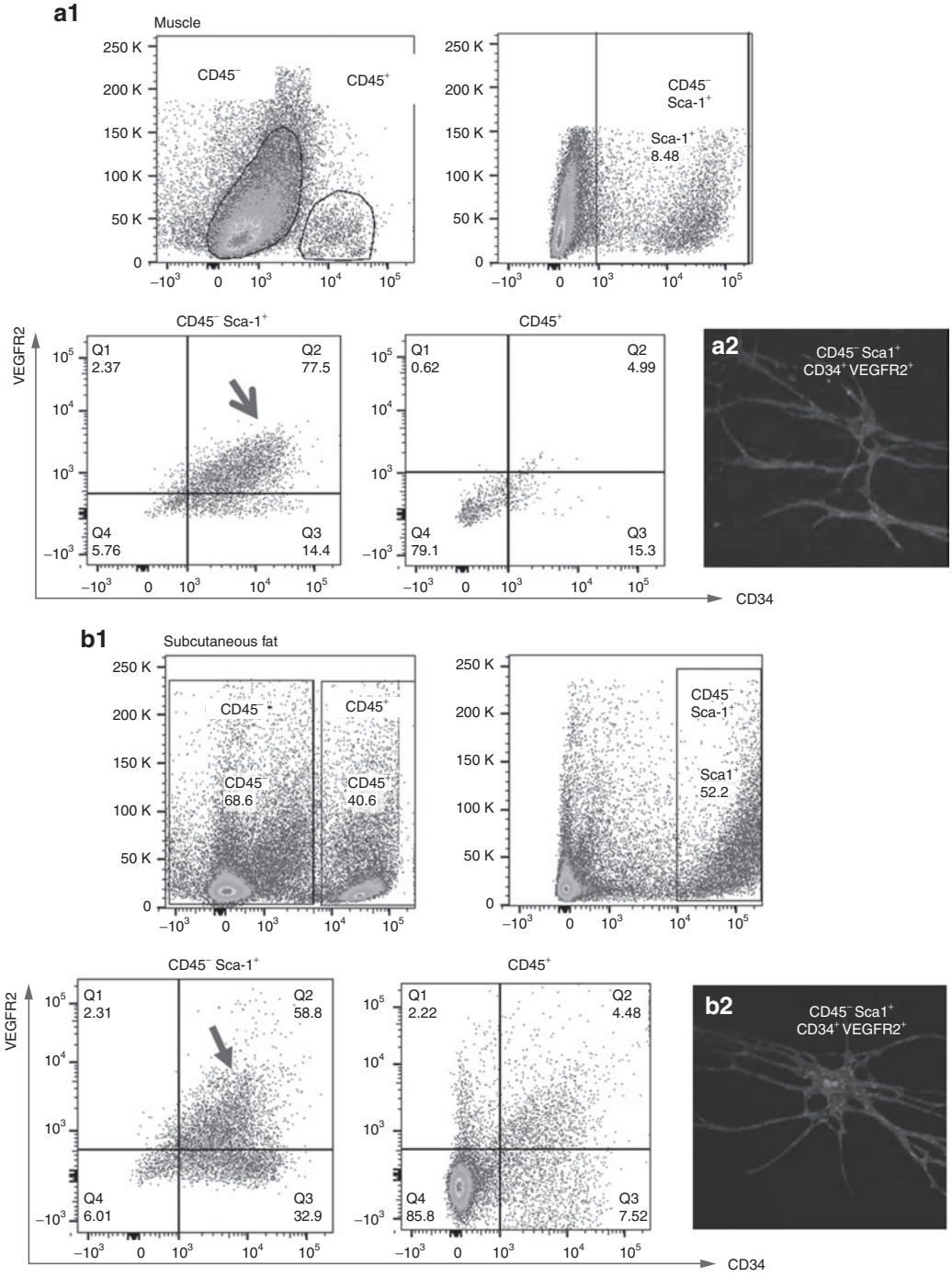

Figure 5 Muscle and subcutaneous fat contain abundant endothelial progenitors. Fluorescence-activated cell sorting (FACS) analyses on mononuclear cells derived from (**a1**) skeletal muscle and (**b1**) subcutaneous fat. Higher percentages of $CD45^{-}Sca\text{-}1^{+}CD34^{+}VEGFR2^{+}$cells (arrows in **a1** and **b1**) were recorded in muscle and fat. Cultures of FACS-sorted $CD45^{-}Sca\text{-}1^{+}CD34^{+}VEGFR2^{+}$ cells from (**a2**) muscle or (**b2**) fat showed robust $CD31^{+}$ microvessel formation.

(**Figure 6**). Furthermore, ShhN overexpression significantly enhanced the formation and morphogenesis of $CD31^{+}$ microvessels in coculture of $CD45^{-}CD34^{+}Sca\text{-}1^{+}$ endothelial progenitors with PDMPCs, demonstrating the advantage of using ShhN-transduced mesenchymal progenitors in revascularization of the scaffold. The data from this study are consistent with those from several recent reports that show a synergistic effect of Shh *in vitro* on osteogenesis and angiogenesis.[37,38]

A marked increase of $TRAP^{+}$ osteoclasts in Ad-ShhN-PDMPC–seeded collagen scaffold at 2 weeks postimplantation was also noticed (**Figure 4**). ShhN overexpression has been shown to increase the OPG/RANKL ratio in bone marrow stromal cells.[39] In this study, we found that Ad-ShhN increased OPG/RANKL ratio by fivefold (data not shown), consistent with the probone formation effects of ShhN on PDMPCs. It has been shown that osteoclasts can be recruited to the scaffold *in vivo* and participate in the resorption

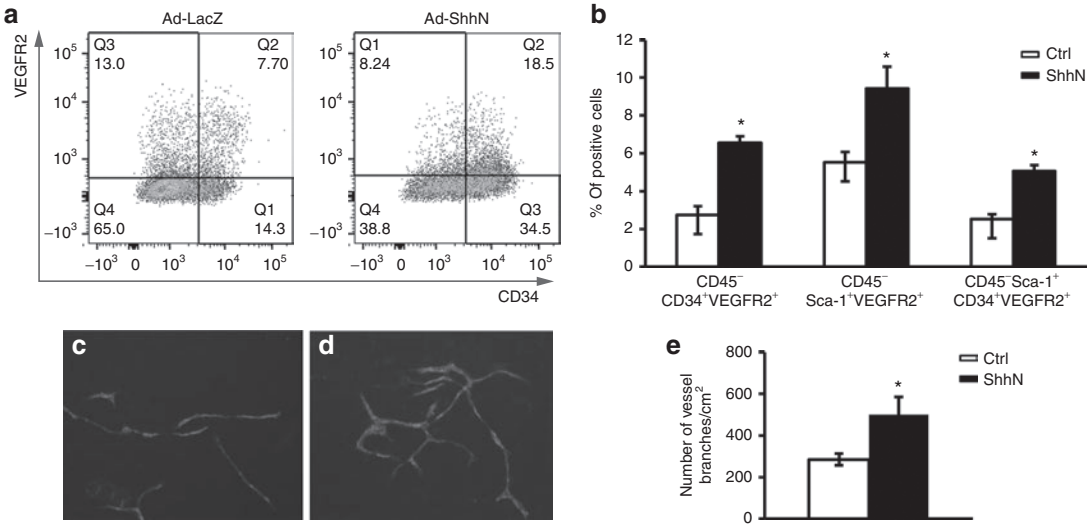

Figure 6 Ad-ShhN-PDMPC collagen scaffold contain more endothelial progenitors at day 7. Cells were isolated from Ad-LaZ-PDMPC-collagen scaffolds or Ad-ShhN-PDMPC-collagen-scaffolds at day 7. (**a**) Ad-ShhN-PDMPC scaffolds contained a higher percentage of $CD45^{-}Sca\text{-}1^{+}CD34^{+}VEGFR2^{+}$ cell population than their respective controls. (**b**) Quantification of the frequencies of $CD45^{-}CD34^{+}VEGFR2^{+}$, $CD45^{-}Sca\text{-}1^{+}VEGFR2^{+}$, and $CD45^{-}Sca\text{-}1^{+}CD34^{+}VEGFR2^{+}$ cells. $n = 3$ per group; $^{*}P < 0.05$. Representative $CD31^{+}$ vessel formation in a coculture of $CD45^{-}Sca1^{+}CD34^{+}$ endothelial progenitors with PDMPCs transduced with (**c**) Ad-LacZ or (**d**) Ad-ShhN. (**e**) Quantitative analyses show more $CD31^{+}$ vessel formation in Ad-ShhN–transduced cells than the respective control cells. $n = 4$ per group; $^{*}P < 0.05$. Ad-GFP, adenovirus-containing GFP; Ad-ShhN, N-terminal sonic hedgehog peptide via an adenoviral vector; Ctrl, control.

of scaffold.[40] Hence, the increased number of $TRAP^{+}$ osteoclasts in collagen scaffold is likely due to the increased neovascularization and enhanced calcification of Ad-ShhN-PDMPC–seeded scaffolds. The increased $TRAP^{+}$ osteoclasts further contribute to the rapid resorption of the collagen scaffold.

Periosteum has been shown to exhibit strong regenerative capacity *in vitro* and *in vivo*.[41,42] *Ex vivo* culture-expanded PDMPCs from human and animals have also been shown to enhance bone formation and bone defect repair.[43,44] However, culture-expanded mesenchymal progenitors often requires seeding on calcium containing scaffold, which could enhance osteogenic differentiation of the seeded cells.[45] Without calcium, one recent report shows that *ex vivo* expanded mesenchymal progenitors, regardless of their sources, have limited advantage in repair of critical bone defect.[46] It is worth noting that a noncalcium-containing collagen sponge was used as scaffold in this study. In these types of nonosteoinductive scaffold, we found only a modest contribution of PDMPCs to cartilage/bone formation at the cortical bone junction in the absence of ShhN, indicating that transplantation of culture-expanded periosteal MPCs alone is not sufficient to induce effective periosteal bone formation. Taken together, our data demonstrate that enhancing the survival and osteogenic differentiation of the donor MPCs and using an adequate osteoinductive scaffold are prerequisites for inducing sufficient bone formation for repair and reconstruction of large bone defects.

In summary, we demonstrate that overexpression of hedgehog agonist ShhN in PDMPCs restores periosteal bone formation in bone allograft transplantation model. The induction of bone formation is donor cell dependent. ShhN further improves host bone formation and host-dependent vascular microenvironment by enhancing endothelial progenitor cell infiltration and rapid revascularization of the scaffold. This study therefore provides strong rationale for the use of Hh agonists in tissue-engineering applications to engender a periosteum replacement for enhanced bone defect repair and reconstruction. Further investigation using immunocompetent mice and large animal models will help in determining the translatability of this study to human.

MATERIALS AND METHODS

Animals and reagents. C57BL/6, GFP transgenic mice were purchased from the Jackson Laboratory (Bar Harbor, Maine). Immunocompromised mice (bg-nu/nu-xid) were purchased from Harlan Sprague Dawley (Frederick, MD). All surgical interventions were approved by the Institutional Animal Care and Use Committee at the University of Rochester. Adenoviruses encoding green fluorescence protein or N-terminal peptide of human Shh (Ad-ShhN) were purified as previously described.[10] Ad-LacZ was purchased from Vector Development Lab at Baylor College of Medicine (Houston, TX).

Segmental bone allograft surgery. A segmental femoral bone allograft transplantation model, described previously,[5,6,23,47] was used to determine the effects of ShhN on bone repair and reconstruction. Briefly, a 10-week-old mouse was anesthetized via intraperitoneal injection of Ketamine and Xylazine. A 4-mm mid-diaphyseal segment was removed from the femur of the donor mice using a sharp diamond-cutting wheel attached to a cordless dremel. A 4-mm devitalized bone allograft was inserted to repair a same sized segmental defect created in mid-diaphyseal region of the mouse femur. The transplanted allograft was stabilized by a 22G stainless pin placed through the intramedullary marrow cavity. All allografts were harvested from 129S1 mice, cleaned, and processed in 75% ethanol to remove cellular debris as previously described.[6] All allografts were stored at −80 °C until use.

Isolation of PDMPCs. To enable tracking of the donor cell fate, PDMPCs were isolated from GFP transgenic mice as previously described.[10,48] Briefly, live bone autograft transplantations were performed in GFP transgenic mice. At least 10 donor autografts were collected at day 5 after transplantation. Periosteum tissues were scraped off and pooled in a Petri dish. After digestion with Collagenase D (Roche Applied Science, Indianapolis, IN) at a concentration of 1 mg/ml for 1 hour, cells released from periosteal tissues were pooled and cultured in α-MEM medium containing 1% penicillin and streptomycin, 1% glutamine, and 20% fetal bovine serum (FBS). Once

confluent, cells were trypsinized and further expanded in α-MEM medium containing 10% FBS. Periosteal cells from fourth and fifth passage were collected and used for all experiments.

Viral transduction and engraftment of PDMPCs around bone allografts. PDMPCs were infected with Ad-GFP or Ad-ShhN at a multiplicity of infection of 100. A total of 1×10^6 cells were seeded onto a collagen scaffold (Cat no. 354613, BD Biosciences, San Jose, CA) and wrapped around a bone allograft. The treated bone allograft was used to repair a 4-mm segmental bone defect created in the immunodeficient mice. A total of 20 immunodeficient mice were split into two experimental groups: allografts treated with Ad-GFP-PDMPCs or allografts treated with Ad-ShhN-PDMPCs. Four animals from each group were harvested at 2-week postsurgery for cell tracking and vascular analyses. The remaining six mice per group were harvested at 6 weeks for histologic and MicroCT analyses.

Histomorphometric analyses of bone graft healing. Paraffin-embedded tissue sections were prepared by H&E/Alcian Blue staining as previously described.[5] Histomorphometric analyses were performed using at least three nonconsecutive sections of each sample, 50 μm apart in the center region of the callus. The percentages of bone, cartilage, and fibrotic tissue formation at the side of donor and host were determined using Osteometrics, which allows interactive tracing of the area of new bone, cartilage, and fibrotic tissue (total callus subtracted from bone and cartilage tissue). A detailed description of the analyses can be found in a previous publication.[23] Briefly, a line was drawn in the middle of the distal or proximal junctions between graft and host bone to separate new bone formation on the surface of the graft and the host bone. Areas of bone, cartilage, and fibrotic tissue on the side of the host or graft were measured separately at both ends to evaluate host and graft bone formation.

Volumetric MicroCT analyses for bone graft healing. Femurs were harvested at 6 weeks and scanned by a Viva MicroCT system (Scanco Medical, Fabrikweg, Switzerland) at a voxel size of 10.5 μm. From the two-dimensional slice images generated, an appropriate threshold was chosen for the bone voxels by visually matching thresholded areas to gray-scale images. Each sample was contoured around the external callus and along the edge of the cortical bone, excluding the marrow cavity. New bone volume was measured on the surface of the host and donor bone, as well as in the total callus in grafted samples as previously described.[6]

Immunohistochemical staining to examine donor cell fate and microvessel formation at the site of repair. Immunohistochemical staining for GFP or CD31 was performed separately on paraffin-embedded tissue sections using a MaxPoly-Two Polymer HRP Mouse Detection Kit (MaxVision Biosciences, Seattle, WA). Primary antibodies for GFP (ab6673) and mouse CD31 (ab28364) were purchased from Abcam (Cambridge, UK) and used in the staining. To determine the number of microvessels in the scaffold region, $CD31^+$ vessels consisting of at least three cells with a lumen structure were counted. The mean of the three nonconsecutive sections from each allograft sample, harvested at 2 weeks after implantation, was used to determine revascularization of the scaffold. At least four allograft samples in each group were used to quantify the number of microvessels per mm^2 area of the scaffold.

Quantitative real-time polymerase chain reaction analyses. Total RNA was prepared using a Qiagen RNA extraction kit. Exactly 0.5 μg of mRNA from four different samples was pooled and reverse transcribed to make single-strand cDNA, using a commercial first strand cDNA synthesis kit (Invitrogen). Quantitative reverse transcriptase–polymerase chain reaction reaction was performed using SyberGreen (ABgene, Rochester, NY) in a RotorGene real time polymerase chain reaction machine (Corbett Research, Carlsbad, CA). All gene expressions were normalized to β-actin and presented as relative to that observed in cells transduced with Ad-GFP or Ad-ShhN. All primers used for the assessment can be found in previous publications.[10,48,49]

Isolation and FACS sorting of endothelial progenitors from skeletal muscle, subcutaneous fat, and bone marrow. Endothelial precursors were isolated from the hind limb skeletal muscle of C57BL6 mice as previously described.[21] Briefly, muscle was minced into small pieces, digested with a final concentration of 2 mg/ml Collagenase type IV (Worthington) supplemented with 2 mM $CaCl_2$ in phosphate buffered saline (PBS) for 45 minutes at 37 °C. To eliminate connective tissue and fibers, samples were passed through 70 and 40 μm nylon cell strainers (BD Falcon, Franklin Lakes, NJ). The stromal vascular fraction of adipose tissue was isolated from subcutaneous fat as described.[50] Bone marrow cells were prepared by flushing the cells from long bone cavity.[5] Mononuclear cells from muscle, fat, and bone marrow were washed, centrifuged, and resuspended in PBS containing 4% FBS for antibody staining. The following antibodies were used for FACS analyses and cell sorting: PerCP conjugated antimouse CD45 (BD Pharmingen, San Jose, CA, Cat no. 557235), phycoerythrin-conjugated antimouse Sca-1 (eBioscience, Cat no. 12-5981-81), allophycocyanin-conjugated antimouse VEGFR2 (eBioscience, Cat no. 12-5921-80), and antimouse CD34 conjugated with Brilliant violet 421(BD Pharmingen, Cat no. 562608). FACS analyses were performed using Canto II flow cytometer. Cell sorting was conducted using a 13-color Aria cell sorter Statler (BioRad, Hercules, CA).

In vitro *microvessel formation assay.* Isolated cells were seeded in Matrigel (R&D) at a density of 5×10^4 in EBM2 media (Lonza, Basel, Switzerland) in 8-well chamber slides (Corning, Corning, NY). The complete EBM2 media supplemented with Lonza growth factor kit including GA100, rhFGF-B, rhEGF, VEGF, IGF1, ascorbic acid, heparin, and FBS were used for microvessel formation assay in Matrigel. After 3–7 days of culture, tube formation was inspected under an inverted light microscope. Isolated cells were also seeded on PDMPC monolayer culture in an 8-well chamber slide (Corning). In the coculture experiments, only basic EBM2 media were used for microvessel formation assays. After 3–7 days of coculture, capillary-like structure could be observed following CD31 immunofluorescent staining.

Immunofluorescent staining of $CD31^+$ vessel formation. Cells in the chamber slides were fixed with cold 4% paraformaldehyde for 1 hour at 4 °C, followed by washing with PBSTX (0.3% triton X-100 in PBS) at room temperature, and blocking with PBSMT (3% BSA in 0.3% PBSTX) for 1 hour at room temperature. The cultures were incubated with antimouse CD31 (BD Pharmingen, Cat no. 553373) overnight followed by extensive wash with 0.3% PBSTX at room temperature. The number of $CD31^+$-positive vessels was counted under a fluorescent microscope (Zeiss Axio Imager, Oberkochen, Germany). The average number of vessel fragments per mm^2 culture area from four samples of each group was calculated and used for statistical analyses. The experiments were repeated three times in PDMPCs.

Analyses of endothelial progenitor cell frequency in collagen scaffold. PDMPCs were isolated from wild-type mice. Cells were infected with control adenovirus Ad-LacZ or Ad-ShhN at a multiplicity of infection of 100. A total of 1×10^6 cells were seeded onto a collagen scaffold and implanted into immunodeficient mice as previously described.[10] Three implants from control and ShhN-treated group were harvested 7 days after surgery. Tissues were minced into small pieces followed by digestion with 2 mg/ml Collagenase type IV (Worthington, Lakewood, NJ). Collected cells were passed through cell restrainers and immediately stained with indicated antibodies for FACS analyses. Frequencies of various populations of cells were analyzed and presented as means of three implants in each treatment group.

Statistical analyses. All data are expressed as a mean value plus or minus the SEM. The statistical significance illustrated in **Figures 1** and **6** between control adenovirus-transduced and Ad-ShhN–transduced PDMPC was determined using Student's *t*-test. The statistical significance illustrated in **Figures 2** and **4** between Ad-GFP-PDMPC– and Ad-ShhN-PDMPC–treated allografts was determined using one-way analysis of variance and a Tukey's *post hoc* test. A P value <0.05 was considered statistically significant. Data analysis was performed using GraphPad Prism version 5.0 (GraphPad Software, San Diego, CA).

SUPPLEMENTARY MATERIAL

Figure S1. Western blot analyses show that PDMPCs transduced with ShhN have higher level of Runx2 protein.

Figure S2. Bone marrow cells contain fewer endothelial progenitors.

Figure S3. Mononuclear cells from adipose tissue or skeletal muscles contained abundant endothelial progenitors.

ACKNOWLEDGMENTS

The authors thank Ryan Tierry, Sarah Mack, and Nehal for their assistance with histological work and Michael Thullen for microCT analyses. This study is supported by grants from the Musculoskeletal Transplant Foundation (X.P.Z.), NYSTEM N08G-495 (X.P.Z.), and N09G346 (X.P.Z.), and the National Institutes of Health (R21 DE021513, RC1AR058435, and AR051469 to X.P.Z.).

REFERENCES

1. Greenwald, AS, Boden, SD, Goldberg, VM, Khan, Y, Laurencin, CT and Rosier, RN; American Academy of Orthopaedic Surgeons. The Committee on Biological Implants (2001). Bone-graft substitutes: facts, fictions, and applications. *J Bone Joint Surg Am* **83-A**(suppl. 2 Pt 2): 98–103.
2. Wheeler, DL and Enneking, WF (2005). Allograft bone decreases in strength *in vivo* over time. *Clin Orthop Relat Res* **435**: 36–42.
3. Sorger, JI, Hornicek, FJ, Zavatta, M, Menzner, JP, Gebhardt, MC, Tomford, WW *et al.* (2001). Allograft fractures revisited. *Clin Orthop Relat Res* **382**: 66–74.
4. Zhang, X, Awad, HA, O'Keefe, RJ, Guldberg, RE and Schwarz, EM (2008). A perspective: engineering periosteum for structural bone graft healing. *Clin Orthop Relat Res* **466**: 1777–1787.
5. Zhang, X, Xie, C, Lin, AS, Ito, H, Awad, H, Lieberman, JR *et al.* (2005). Periosteal progenitor cell fate in segmental cortical bone graft transplantations: implications for functional tissue engineering. *J Bone Miner Res* **20**: 2124–2137.
6. Xie, C, Reynolds, D, Awad, H, Rubery, PT, Pelled, G, Gazit, D *et al.* (2007). Structural bone allograft combined with genetically engineered mesenchymal stem cells as a novel platform for bone tissue engineering. *Tissue Eng* **13**: 435–445.
7. Zou, XH, Cai, HX, Yin, Z, Chen, X, Jiang, YZ, Hu, H *et al.* (2009). A novel strategy incorporated the power of mesenchymal stem cells to allografts for segmental bone tissue engineering. *Cell Transplant* **18**: 433–441.
8. Zhao, L, Zhao, J, Wang, S, Xia, Y, Liu, J, He, J *et al.* (2011). Evaluation of immunocompatibility of tissue-engineered periosteum. *Biomed Mater* **6**: 015005.
9. Zhao, L, Zhao, J, Wang, S, Wang, J and Liu, J (2011). Comparative study between tissue-engineered periosteum and structural allograft in rabbit critical-sized radial defect model. *J Biomed Mater Res Part B Appl Biomater* **97**: 1–9.
10. Wang, Q, Huang, C, Zeng, F, Xue, M and Zhang, X (2010). Activation of the Hh pathway in periosteum-derived mesenchymal stem cells induces bone formation in vivo: implication for postnatal bone repair. *Am J Pathol* **177**: 3100–3111.
11. Ingham, PW and McMahon, AP (2001). Hedgehog signaling in animal development: paradigms and principles. *Genes Dev* **15**: 3059–3087.
12. Shimoyama, A, Wada, M, Ikeda, F, Hata, K, Matsubara, T, Nifuji, A *et al.* (2007). Ihh/Gli2 signaling promotes osteoblast differentiation by regulating Runx2 expression and function. *Mol Biol Cell* **18**: 2411–2418.
13. Patel-Hett, S and D'Amore, PA (2011). Signal transduction in vasculogenesis and developmental angiogenesis. *Int J Dev Biol* **55**: 353–363.
14. Dyer, MA, Farrington, SM, Mohn, D, Munday, JR and Baron, MH (2001). Indian hedgehog activates hematopoiesis and vasculogenesis and can respecify prospective neurectodermal cell fate in the mouse embryo. *Development* **128**: 1717–1730.
15. Vokes, SA, Yatskievych, TA, Heimark, RL, McMahon, J, McMahon, AP, Antin, PB *et al.* (2004). Hedgehog signaling is essential for endothelial tube formation during vasculogenesis. *Development* **131**: 4371–4380.
16. Moran, CM, Myers, CT, Lewis, CM and Krieg, PA (2012). Hedgehog regulates angiogenesis of intersegmental vessels through the VEGF signaling pathway. *Dev Dyn* **241**: 1034–1042.
17. Lavine, KJ, Kovacs, A and Ornitz, DM (2008). Hedgehog signaling is critical for maintenance of the adult coronary vasculature in mice. *J Clin Invest* **118**: 2404–2414.
18. Straface, G, Aprahamian, T, Flex, A, Gaetani, E, Biscetti, F, Smith, RC *et al.* (2009). Sonic hedgehog regulates angiogenesis and myogenesis during post-natal skeletal muscle regeneration. *J Cell Mol Med* **13**(8B): 2424–2435.
19. Pola, R, Ling, LE, Aprahamian, TR, Barban, E, Bosch-Marce, M, Curry, C *et al.* (2003). Postnatal recapitulation of embryonic hedgehog pathway in response to skeletal muscle ischemia. *Circulation* **108**: 479–485.
20. Palladino, M, Gatto, I, Neri, V, Straino, S, Silver, M, Tritarelli, A *et al.* (2011). Pleiotropic beneficial effects of sonic hedgehog gene therapy in an experimental model of peripheral limb ischemia. *Mol Ther* **19**: 658–666.
21. Ieronimakis, N, Balasundaram, G and Reyes, M (2008). Direct isolation, culture and transplant of mouse skeletal muscle derived endothelial cells with angiogenic potential. *PLoS ONE* **3**: e0001753.
22. Martin-Padura, I, Gregato, G, Marighetti, P, Mancuso, P, Calleri, A, Corsini, C *et al.* (2012). The white adipose tissue used in lipotransfer procedures is a rich reservoir of CD34+ progenitors able to promote cancer progression. *Cancer Res* **72**: 325–334.
23. Tiyapatanaputi, P, Rubery, PT, Carmouche, J, Schwarz, EM, O'keefe, RJ and Zhang, X (2004). A novel murine segmental femoral graft model. *J Orthop Res* **22**: 1254–1260.
24. Hu, H, Hilton, MJ, Tu, X, Yu, K, Ornitz, DM and Long, F (2005). Sequential roles of Hedgehog and Wnt signaling in osteoblast development. *Development* **132**: 49–60.
25. Long, F, Chung, UI, Ohba, S, McMahon, J, Kronenberg, HM and McMahon, AP (2004). Ihh signaling is directly required for the osteoblast lineage in the endochondral skeleton. *Development* **131**: 1309–1318.
26. Lou, H, Crystal, RG and Leopold, PL (2005). Enhanced efficacy of cholesterol-minus sonic hedgehog in postnatal skin. *Mol Ther* **12**: 575–578.
27. Ishihara, A, Zekas, LJ, Weisbrode, SE and Bertone, AL (2010). Comparative efficacy of dermal fibroblast-mediated and direct adenoviral bone morphogenetic protein-2 gene therapy for bone regeneration in an equine rib model. *Gene Ther* **17**: 733–744.
28. Li, R, Stewart, DJ, von Schroeder, HP, Mackinnon, ES and Schemitsch, EH (2009). Effect of cell-based VEGF gene therapy on healing of a segmental bone defect. *J Orthop Res* **27**: 8–14.
29. Coultas, L, Nieuwenhuis, E, Anderson, GA, Cabezas, J, Nagy, A, Henkelman, RM *et al.* (2010). Hedgehog regulates distinct vascular patterning events through VEGF-dependent and -independent mechanisms. *Blood* **116**: 653–660.
30. Lavine, KJ, White, AC, Park, C, Smith, CS, Choi, K, Long, F *et al.* (2006). Fibroblast growth factor signals regulate a wave of Hedgehog activation that is essential for coronary vascular development. *Genes Dev* **20**: 1651–1666.
31. Pola, R, Ling, LE, Silver, M, Corbley, MJ, Kearney, M, Blake Pepinsky, R *et al.* (2001). The morphogen Sonic hedgehog is an indirect angiogenic agent upregulating two families of angiogenic growth factors. *Nat Med* **7**: 706–711.
32. Fagiani, E and Christofori, G (2013). Angiopoietins in angiogenesis. *Cancer Lett* **328**: 18–26.
33. Felcht, M, Luck, R, Schering, A, Seidel, P, Srivastava, K, Hu, J *et al.* (2012). Angiopoietin-2 differentially regulates angiogenesis through TIE2 and integrin signaling. *J Clin Invest* **122**: 1991–2005.
34. Lee, HJ, Cho, CH, Hwang, SJ, Choi, HH, Kim, KT, Ahn, SY *et al.* (2004). Biological characterization of angiopoietin-3 and angiopoietin-4. *FASEB J* **18**: 1200–1208.
35. Fu, JR, Liu, WL, Zhou, JF, Sun, HY, Xu, HZ, Luo, L *et al.* (2006). Sonic hedgehog protein promotes bone marrow-derived endothelial progenitor cell proliferation, migration and VEGF production via PI 3-kinase/Akt signaling pathways. *Acta Pharmacol Sin* **27**: 685–693.
36. Asai, J, Takenaka, H, Kusano, KF, Ii, M, Luedemann, C, Curry, C *et al.* (2006). Topical sonic hedgehog gene therapy accelerates wound healing in diabetes by enhancing endothelial progenitor cell-mediated microvascular remodeling. *Circulation* **113**: 2413–2424.
37. Dohle, E, Fuchs, S, Kolbe, M, Hofmann, A, Schmidt, H and Kirkpatrick, CJ (2010). Sonic hedgehog promotes angiogenesis and osteogenesis in a coculture system consisting of primary osteoblasts and outgrowth endothelial cells. *Tissue Eng Part A* **16**: 1235–1237.
38. Rivron, NC, Raiss, CC, Liu, J, Nandakumar, A, Sticht, C, Gretz, N *et al.* (2012). Sonic Hedgehog-activated engineered blood vessels enhance bone tissue formation. *Proc Natl Acad Sci USA* **109**: 4413–4418.
39. Kiuru, M, Solomon, J, Ghali, B, van der Meulen, M, Crystal, RG and Hidaka, C (2009). Transient overexpression of sonic hedgehog alters the architecture and mechanical properties of trabecular bone. *J Bone Miner Res* **24**: 1598–1607.
40. Kagawa, R, Kishino, M, Sato, S, Ishida, K, Ogawa, Y, Ikebe, K *et al.* (2012). Chronological histological changes during bone regeneration on a non-crosslinked atelocollagen matrix. *J Bone Miner Metab* **30**: 638–650.
41. Stevens, MM, Marini, RP, Schaefer, D, Aronson, J, Langer, R and Shastri, VP (2005). *In vivo* engineering of organs: the bone bioreactor. *Proc Natl Acad Sci USA* **102**: 11450–11455.
42. Gallay, SH, Miura, Y, Commisso, CN, Fitzsimmons, JS and O'Driscoll, SW (1994). Relationship of donor site to chondrogenic potential of periosteum *in vitro*. *J Orthop Res* **12**: 515–525.
43. van Gastel, N, Torrekens, S, Roberts, SJ, Moermans, K, Schrooten, J, Carmeliet, P *et al.* (2012). Engineering vascularized bone: osteogenic and proangiogenic potential of murine periosteal cells. *Stem Cells* **30**: 2460–2471.
44. Roberts, SJ, Geris, L, Kerckhofs, G, Desmet, E, Schrooten, J and Luyten, FP (2011). The combined bone forming capacity of human periosteal derived cells and calcium phosphates. *Biomaterials* **32**: 4393–4405.
45. Yuan, H, Fernandes, H, Habibovic, P, de Boer, J, Barradas, AM, de Ruiter, A *et al.* (2010). Osteoinductive ceramics as a synthetic alternative to autologous bone grafting. *Proc Natl Acad Sci USA* **107**: 13614–13619.
46. Stockmann, P, Park, J, von Wilmowsky, C, Nkenke, E, Felszeghy, E, Dehner, JF *et al.* (2012). Guided bone regeneration in pig calvarial bone defects using autologous mesenchymal stem/progenitor cells - a comparison of different tissue sources. *J Craniomaxillofac Surg* **40**: 310–320.
47. Koefoed, M, Ito, H, Gromov, K, Reynolds, DG, Awad, HA, Rubery, PT *et al.* (2005). Biological effects of rAAV-caAlk2 coating on structural allograft healing. *Mol Ther* **12**: 212–218.
48. Wang, Q, Huang, C, Xue, M and Zhang, X (2011). Expression of endogenous BMP-2 in periosteal progenitor cells is essential for bone healing. *Bone* **48**: 524–532.
49. Dhillon, RS, Xie, C, Tyler, W, Calvi, LM, Awad, HA, Zuscik, MJ *et al.* (2013). PTH-enhanced structural allograft healing is associated with decreased angiopoietin-2-mediated arteriogenesis, mast cell accumulation, and fibrosis. *J Bone Miner Res* **28**: 586–597.
50. Koh, YJ, Koh, BI, Kim, H, Joo, HJ, Jin, HK, Jeon, J *et al.* (2011). Stromal vascular fraction from adipose tissue forms profound vascular network through the dynamic reassembly of blood endothelial cells. *Arterioscler Thromb Vasc Biol* **31**: 1141–1150.